# Comparison Between Newmark Time History Analysis and Finite Element Method for Estimating Seismically Induced Slope Displacement

Mahir Badanagki[1](✉), Feng Li[2], and Christian Armstrong[3]

[1] WSP/GOLDER, 7245 W Alaska Drive, Suite, 200, Lakewood, CO, USA
mahir.badanagki@wsp.com
[2] WSP/GOLDER, 18300 NE Union Hill Road, Suite 200, Redmond, WA 98052, USA
feng.li@wsp.com
[3] WSP/GOLDER, 7245 W Alaska Drive, Suite 200, Lakewood, CO 80226, USA
Christian.armstrong@wsp.com

**Abstract.** Estimating the seismically induced slope displacement is important in assessing the stability and relative deformation of slopes during earthquakes. The Newmark time history analysis (also known as Newmark displacement analysis) bridges the gap between the simplified pseudo-static method and complex stress-deformation analysis such as finite element (FE) analysis. However, the Newmark time history analysis may result in smaller dynamic deformation estimates. There is a lack of guidance on if the same deformation performance criterion should be applied to all methods. The study is divided into three parts: First, a two-dimensional stability analysis of the study slope was carried out for static and pseudo-static loading conditions per the relevant standard guidelines. Slope deformation was estimated for the pseudo-static loading condition using the simplified, empirical Bray and Macedo's (2019) method for horizontal vibrations and shallow crustal earthquakes. Then, Newmark displacement of the slope along its most probable failure surface was estimated for selected earthquake time histories using the SLAMMER code built into the Slide2 software. Both coupled/decoupled acceleration time history methods were carried out. In the final part, finite element analysis was conducted for the same slope using the same earthquake time histories. Comparison of slope displacements at the crest from these three methods show that seismically induced displacements estimated using the Newmark time history analysis can be smaller than those from the FE analysis. Recommendations for building case study pools and developing method-dependent performance criteria are also included.

**Keywords:** Seismic stability · Newmark · Displacement

## 1 Introduction

Failure of engineered and natural slopes during earthquakes has attracted considerable attention from many researchers to work on slope stability analysis. The approach to evaluate the slope stability under seismic loading can be divided into three main categories:

S. Javankhoshdel and Y. Abolfazlzadeh (Eds.): TMIC 2022, AHE 13, pp. 171–178, 2023.
https://doi.org/10.2991/978-94-6463-104-3_16

pseudo-static methods (e.g., Terzaghi 1950; Sarma and Bhave 1974; Bray and Macedo 2019), Newmark sliding block method (e.g., Newmark 1965), and stress-deformation analysis (e.g., Seed et al. 1975).

The pseudo-static methods first use two-dimensional (2D) limit equilibrium (LE) analyses to estimate the yield acceleration for which the factor of safety equals unity. The pseudo-static methods then use empirical relationships, which are functions of the yield acceleration, moment earthquake magnitude, and response spectral acceleration and were developed based on observations from historical events, to estimate slope seismic displacements. However, the pseudo-static methods do not use earthquake acceleration time histories (EATHs) as inputs.

The Newmark method can determine the permanent displacement of the slope during an earthquake using earthquake acceleration time histories as inputs. For this method, deformations where the acceleration exceeds the yield acceleration along the critical slip surface are summed.

Finally, dynamic finite-element (FE) or finite-difference (FD) analyses can obtain the stress and strain results of the slopes induced by earthquakes by incorporating dynamic properties and earthquake acceleration time histories.

Out of these three approaches, the FE or FD analyses typically have longer analysis time, require more field and laboratory investigations to calibrate selected soil dynamic constitutive models, hence are significantly more expensive, whereas simplified pseudo-static analyses are typically the standard screening tool. Therefore, the Newmark method bridges the gap between the simplified pseudo-static method and complicated stress-deformation analysis.

For this study, permanent-displacement analyses under seismic loading were completed for an in-pit dump slope using a simplified pseudo-static method (i.e., Bray and Macedo 2019), a Newmark method (i.e., SLAMMER), and a 2D FE analysis. The steps for performing these analyses include:

1. Develop EATHs for the site-specific target acceleration response spectrum and for representative earthquakes. The target spectrum is the uniform hazard response spectrum with an annual exceedance probability of 1 in 475 years. The EATHs were developed using the amplitude scaling method.
2. Perform a 2D LE stability analysis using the Morgenstern and Price method to estimate the global safety factor for the slope under the static loading and the yield acceleration under dynamic loading.
3. Perform simplified pseudo-static and Newmark time-history analysis using SLAMMER.
4. Perform dynamic FE deformation analysis using a 2D geotechnical FE analysis software RS2 from Rocscience.
5. Compare the results from the above analyses.

## 2 Material Properties

Before performing the seismic stability analyses, material properties were selected based on field investigations and observations, laboratory testing, and experience with similar

**Table 1.** Summary of strength parameters for in-pit dump materials

| Material | Unit Weight (kN/m$^3$) | Poisson's Ratio | Young's Modulus (kPa) | Friction Angle (°) | Cohesion (kPa) |
|---|---|---|---|---|---|
| Arkose | 21.4 | 0.3 | 136,555 | 33.9 | 0 |
| Upper Lakebed Clays | 20.6 | 0.3 | 37,921 | 10.5 | 0 |
| Lakebed Clays | 20.6 | 0.3 | 489,768 | 10.5 | 0 |
| Ore | 17.9 | 0.3 | 37,921 | 28 | 553 |
| Basalt | 23.6 | 0.35 | 7,218,578 | 29 | 310 |
| Arkose Dump | 18.9 | 0.3 | 127,409 | 34 | 0 |
| Lower Tropico Clay | 21.4 | 0.3 | 42,183 | 14 | 148 |
| Lower Tropico | 21.4 | 0.35 | 136,555 | 34 | 666 |

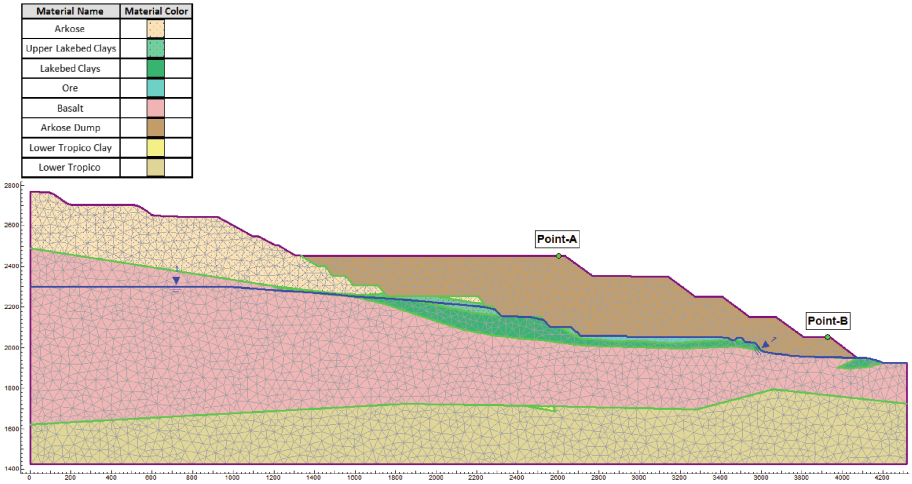

**Fig. 1.** Slope geometry and finite element mesh

materials. The cross-section of the slope is shown in Fig. 1. The dump slope height is approximately 122 m. Table 1 lists the material properties used in this study.

## 3 Simplified Deformation Analysis

A simplified deformation analysis was first carried out and consisted of three steps.

1. First, a static stability analysis was completed using the Slide2 program from Rocscience (Rocscience 2021), which incorporates various well-established and popular limit equilibrium (LE) methods for 2D stability assessment. For the present study,

the Morgenstern and Price method was used to estimate the global safety factor for the slope under static loading.

2. Pseudo-static seismic analyses were then performed in Slide2 to estimate the yield acceleration, $k_y$, which is the horizontal seismic coefficient that results in a factor of safety of 1.0 using the seismic strengths of the materials.
3. Next, a simple deformation analysis using the Bray and Macedo (2019) empirical equation was used to estimate the displacement at the crest of the slope due to shear deformation. The direction of this displacement is in parallel to the direction of slope movement. The Bray and Macedo (2019) empirical equation was developed based on observations from previous seismic events. The Bray and Macedo (2019) empirical equation is a function of the yield acceleration, moment magnitude of the earthquake, the fundamental period of the failing mass, and the spectral acceleration at 1.2 times the fundamental period. The results of the simplified deformation analysis are listed in Table 3.

## 4 Earthquake Acceleration Time History Development

Ten, single-component EATHs were developed for the target, site-specific response spectrum for the selected design earthquake. The target spectrum is the uniform hazard response spectrum with an annual exceedance probability of 1 in 475 years. The EATHs were developed using the amplitude scaling method. Seed EATHs were selected from the Pacific Earthquake Engineering Research Center (PEER) Next Generation Attenuation

**Table 2.** Key parameters of selected and scaled EATHs

| **RSN(a)** | **Moment Magnitude (Mw)** | **Year** | **Scale Factor** | **$R_{rup}$(b) (km)** | **$R_{jb}$(c) (km)** | **$V_{S30}$(d) (m/s)** | **$D_{5–75}$(e) (s)** | **$D_{5–95}$(f) (s)** | **Scaled AI(g) (m/s)** |
|---|---|---|---|---|---|---|---|---|---|
| 1005 | 6.69 | 1994 | 1.80 | 31 | 29 | 452 | 7.3 | 14.6 | 1.1 |
| 1083 | 6.69 | 1994 | 1.79 | 13 | 12 | 402 | 6.8 | 15.9 | 1.1 |
| 4841 | 6.80 | 2007 | 1.49 | 26 | 21 | 655 | 7.1 | 15.8 | 0.9 |
| 4854 | 6.80 | 2007 | 2.15 | 36 | 36 | 571 | 7.0 | 21.1 | 0.9 |
| 15 | 7.36 | 1952 | 1.51 | 39 | 38 | 385 | 10.2 | 28.8 | 1.4 |
| 143 | 7.35 | 1978 | 0.32 | 2 | 2 | 767 | 8.3 | 16.5 | 1.2 |
| 3746 | 7.01 | 1992 | 0.67 | 18 | 16 | 459 | 4.3 | 10.4 | 0.7 |
| 1284 | 7.62 | 1999 | 3.50 | 48 | 44 | 677 | 11.4 | 22.0 | 1.4 |
| 1474 | 7.62 | 1999 | 3.53 | 53 | 52 | 665 | 12.7 | 18.2 | 1.3 |
| 1177 | 7.51 | 1999 | 1.97 | 54 | 52 | 342 | 17.7 | 39.4 | 1.0 |

a. The record sequence number is assigned to individual records in the PEER NGA-West2 database.
b. $R_{rup}$ = closest distance to fault rupture.
c. $R_{jb}$ = closest horizontal distance to the projected fault rupture.
d. $V_{s30}$ = the time-averaged shear-wave velocity for the upper 30 m of earth materials below the ground surface.
e. $D_{5–75}$ = significant duration; the time between 5% and 75% of the cumulative Arias intensity.
f. $D_{5–95}$ = significant duration; the time between 5% and 95% of the cumulative Arias intensity.
g. AI = Arias intensity.

Phase 2 Project (NGA-West2) strong-motion database. Table 2 lists key parameters of the selected and scaled EATHs.

## 5 Newmark Time History Analysis

Another method to estimate permanent slope displacement is the Newmark time history analysis. The principle of a Newmark time history analysis is that, during an earthquake, there will be short moments in time when the inertial forces plus the initial static forces will exceed the available shear resistance, resulting in temporary loss of stability and unrecoverable deformations. These unrecoverable deformations will then result in a permanent deformation at the conclusion of the seismic event.

For the present study, the Newmark time history analysis was performed in Slide2 which uses the program SLAMMER (seismic landslide movement modeled using earthquake records), developed by U.S. Geological Survey. SLAMMER calculates the cumulative displacement via double integration of an earthquake acceleration time history. First, the acceleration time history is reduced to only the parts above the critical, or yield, acceleration from 2D LE stability analyses. These parts are then integrated to obtain the respective velocity and displacement time histories. The permanent displacement equals the cumulative displacements to the end of the time history. To perform the analysis, SLAMMER requires an acceleration time history and the yield acceleration to estimate the seismic displacement.

The permanent displacement values obtained from the Newmark time history analyses for ten earthquake acceleration time histories are shown in Table 3. The displacements were estimated along the critical slip surfaces according to the corresponding 2D LE stability analyses. The direction of the displacements is parallel to the direction of slope movement.

**Table 3.** Summary of dynamic deformation results

| **Record Sequence Number** | **Finite Element Method** | | | | **SLAMMER** | **Simplified Method** (Bray and Macedo 2019) |
|---|---|---|---|---|---|---|
| | **Point A** | | **Point B** | | | |
| | **Vertical Displacement (m)** | **Horizontal Displacement (m)** | **Vertical Displacement (m)** | **Horizontal Displacement (m)** | **Displacement (m)** | **Displacement (m)** |
| 1005 | -0.12 | 0.31 | -0.13 | 0.24 | 0.17 | 0.29 |
| 1083 | -0.14 | 0.34 | -0.16 | 0.30 | 0.26 | |
| 1177 | -0.24 | 0.77 | -0.37 | 0.69 | 0.23 | |
| 1284 | -0.19 | 0.76 | -0.22 | 0.60 | 0.26 | |
| 143 | -0.15 | 0.40 | -0.16 | 0.33 | 0.20 | |
| 1474 | -0.25 | 0.97 | -0.30 | 0.84 | 0.32 | |
| 15 | -0.19 | 0.53 | -0.20 | 0.41 | 0.23 | |
| 3746 | -0.12 | 0.34 | -0.12 | 0.24 | 0.24 | |
| 4841 | -0.12 | 0.33 | -0.15 | 0.28 | 0.17 | |
| 4854 | -0.12 | 0.36 | -0.14 | 0.27 | 0.16 | |
| Average | -0.16 | 0.51 | -0.20 | 0.42 | 0.22 | |

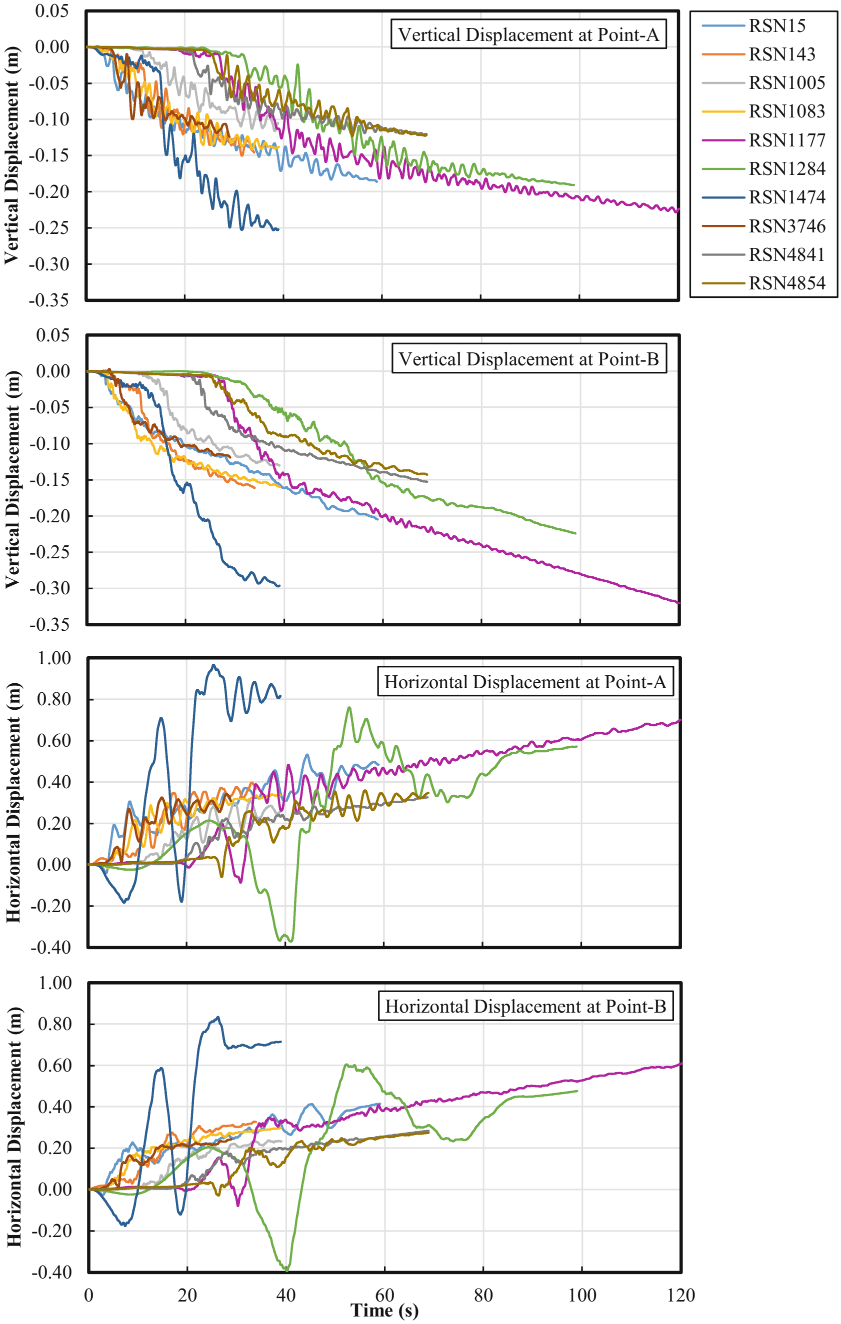

**Fig. 2.** Vertical and horizontal displacements for RSN 15, 143, 1005, 1083, 1177, 1284, 1474, 3746, 4841, and 4854 at Point A and B from dynamic FE deformation analysis

## 6 Finite Element Analysis

Dynamic deformation analyses were completed using 2D FE analysis software RS2 from Rocscience. Figure 1 presents the analyzed section with two points that typically are critical for these analyses: Point A at the crest and Point B at the toe. Graphical plots of estimated horizontal and vertical displacements at each point are shown in Fig. 2. Vertical and horizontal strains were estimated using the estimated permanent displacements at the end of the earthquake shaking from RS2, where the vertical strain is the vertical displacement divided by the failure mass height (122 m) and the horizontal strain is the horizontal displacement divided by the failure mass length (588 m). Compliant base boundary condition was assigned at the base of the FE model to absorb the downward waves while transmitting boundary conditions were assigned to the lateral sides.

Figure 2 summarized the combined slope displacements from horizontal and vertical displacements from the dynamic deformation analyses. Both the slope displacements from individual motions and the arithmetic average were listed. Table 3 shows that the average displacement estimate from the Newmark method is the smallest among the three methods and the average displacement from the FE method is the largest.

The results from the analytical methods were compared to acceptable deformations from literature (Hawley and Cunning 2017). The results of the dynamic FE deformation modeling indicate that the maximum estimated strain on the dump slope is approximately 0.31% which occurs at the dump toe at Point B. The estimated maximum strain is less than 0.5% which is the most conservative maximum allowable strain for a high consequence dump with low confidence in the material properties (Hawley and Cunning 2017). These results indicate that the performance of the analyzed waste dump slope meets the acceptable deformations. The other methods also result in acceptable deformations of the dump slope.

## 7 Conclusion

Three methods were evaluated to estimate seismic displacements, including a simplified method that uses a yield acceleration and an empirical equation (Bray and Macedo 2019), a Newmark time history method (using SLAMMER), and a dynamic FE deformation analysis. Results show that the deformations calculated using SLAMMER and Bray and Macedo (2019) are smaller than those estimated by the FE modeling. For the slope of interest, the estimated strain from all three analyses are smaller than the suggested acceptance criteria presented in Guidelines for Mine Waste Dump and Stockpile Design (Hawley and Cunning 2017). Hence, using either of the three methods, the same conclusion that the performance of the analyzed waste dump slope satisfactorily meets the guidelines can be reached.

There, however, may be cases for which the simplified method and the Newmark time history method result in acceptable small permanent displacements, whereas the FE method results in a permanent displacement greater than the acceptance criterion. For these cases, we may reach a different conclusion without doing the more expensive and time-consuming FE analysis. We, therefore, recommend building a pool of case studies and, if warranted, developing method-dependent performance criteria. For example, if the pool of case studies shows that the simplified methods more likely result in smaller displacements, maybe the performance criteria for the simplified methods need to be more stringent than those for the FE methods. This pool of case studies should be based on results from a variety of waste dump slopes using a range of earthquake records.

Additionally, future waste dumps in high seismicity regions should be instrumented with a variety of sensors to evaluate deformations during seismic events. These measurements are critical to validate both the performance of the facilities as well as be back analyzed and compared to results from the predictive methods.

## References

Bray JD, Macedo J., Procedure for estimating shear-induced seismic slope displacement for Shallow Crustal Earthquakes. J Geotech Geoenviron Eng 145(12) (2019).

Hawley and Cunning., Guidelines for Mine Waste Dump and Stockpile Design. CSIRO Publishing. Clayton South VIC, Australia. (2017).

Jibson, R. W., Rathje, E. M., Jibson, M. W., and Lee, Y. W. “SLAMMER-Seismic landslide movement modeled using earthquake records.” Techniques and Methods 12-B1, USGS, Reston, VA. (2013).

Rocscience Inc. Slide2 Version 9.015. Toronto, Ontario, Canada (2021).

Sarma SK and Bhave MV. Critical Acceleration Versus Static Factor of Safety in Stability Analysis of Earth Dams and Embankments. Géotechnique, 24(4): 661–665 (1974).

Seed HB, Idriss IM, Lee KL and Makdisi FI. Dynamic Analysis of the Slide in the Lower San Fernando Dam during the Earthquake of February 9, 1971. Journal of Geotechnical and Geoenvironmental Engineering, 101(9): 889–911 (1975).

Terzaghi K, Mechanisms of landslides. Engineering Geology (Berkey) Volume, Geological Society of America (1950).

Newmark NM. Effects of Earthquakes on Dams and Embankments. Géotechnique, 15(2): 139–160 (1965).